

# Dynamical transition in a jammed state of a quasi-two-dimensional foam

Rei Kurita,<sup>1</sup> Yujiro Furuta,<sup>1,2</sup> Naoya Yanagisawa,<sup>1</sup> and Noriko Oikawa<sup>1</sup>

<sup>1</sup>*Department of Physics, Tokyo Metropolitan University, Minamiosawa, Hachioji-shi, Tokyo 192-0397, Japan*

<sup>2</sup>*Department of Physics, Tokyo Institute of Technology, Ookayama, Meguro-ku, Tokyo 152-8551, Japan*

(Received 3 April 2017; revised manuscript received 22 May 2017; published 30 June 2017)

The states of foam are empirically classified into dry foam and wet foam by the volume fraction of the liquid. Recently, a transition between the dry foam state and the wet foam state has been found by characterizing the bubble shapes [Furuta *et al.*, *Sci. Rep.* **6**, 37506 (2016)]. In the literature, it is indirectly ascertained that the transition from the dry to the wet form is related to the onset of the rearrangement of the bubbles, namely, the liquid fraction at which the bubbles become able to move to replace their positions. The bubble shape is a static property, and the rearrangement of the bubbles is a dynamic property. Thus, we investigate the relation between the bubble shape transition and the rearrangement event occurring in a collapsing process of the bubbles in a quasi-two-dimensional foam system. The current setup brings a good advantage to observe the above transitions, since the liquid fraction of the foam continuously changes in the system. It is revealed that the rearrangement of the bubbles takes place at the dry-wet transition point where the characteristics of the bubble shape change.

DOI: [10.1103/PhysRevE.95.062613](https://doi.org/10.1103/PhysRevE.95.062613)

## I. INTRODUCTION

Liquid-gas foam is a state composed of gas bubbles and liquid films. The unique mechanical properties of the foam, which is associated with the cell structure of the gas bubbles, lead to a wide variety of applications, such as heat insulating materials, drying preventions, and antioxidation. The foam shows macroscopic elasticity, despite the fact that both the gas and the liquid phases are fluids. The elastic properties come from the jamming state of the bubbles, and the foam has been intensively studied as a soft jammed system [1–6]. The jamming transition in the foam system occurs at the liquid fraction  $\phi \approx 0.36$  in three-dimensional foam ( $\phi_{2D} \approx 0.16$  in two-dimensional foam). The values of  $\phi$  are consistent with the liquid fraction of random close packing in granular systems [7–10]. Much of the research on the foam system has been dedicated to the critical phenomena observed near the jamming transition point [6,11]. In the region of  $\phi$  far below the jamming transition point, the foam is empirically classified into two states, the dry foam and the wet foam [12–16]. In three-dimensional foam, the shape of the bubbles is polyhedral when  $\phi$  is below 0.05 and the state is called the dry foam. Meanwhile, the system is in the wet foam state when  $\phi$  is above 0.15 and the shape of the bubbles becomes spherical. In the past experimental study, it was shown that the configuration of the bubbles is bcc in the dry foam, while it is fcc in the wet foam for monodispersed foam systems [17]. Another study found that the coarsening process of the bubble in the dry foam was different from that in the wet foam [18]. The rheology of the wet foam and the dry foam has been studied both experimentally and numerically [19–22]. However, the difference between the wet foam and the dry foam has still been unclear in the polydispersed foam. Thus fundamental understandings of the physical properties of the foam is still lacking, although the importance of the foam is widely recognized [19,23,24].

Dynamical properties of the foam have been also investigated [25,26]. Jamming and flow properties of random close-packed spherical bubbles are governed by osmotic pressure  $p$  near the jamming point [25]. The bubble rearrangement duration also depends on  $p$  rather than  $\phi$  for  $\phi > 0.08$  [26].

However, the relation between  $\phi$  and  $p$ , and the rearrangement of the bubbles for lower  $\phi$  is still unclear.

Recently, we have investigated the shape change of the bubbles in a collapsing process of the bubbles in a quasi-two-dimensional foam system [27]. In the collapsing process of the bubbles  $\phi$  continuously increases with time, which enables us to follow the shape change of the bubbles throughout a wide range of  $\phi$ . We found two transitions in the bubble shape in the region far below the jamming point, which means that three states clearly exist in the foam system. We called those states superdry foam, dry foam, and wet foam in order from lower  $\phi$ . We also suggested that the rearrangement of the bubbles starts to occur at the transition point from the dry foam to the wet foam by investigating the whole shape of the foam. However, the rearrangement is a dynamical property, while the whole shape of the foam is a static property. Thus the investigation of the dynamics is needed to ascertain the relation between the dry-wet transition and the rearrangement. Furthermore,  $\phi_{2D}$  at the final state ( $\sim 0.5$ ) is much larger than  $\phi_{2D}$  at the jamming transition in a two-dimensional system ( $\phi_{2D} \approx 0.16$ ). Since the experiment is extended in a wide range of  $\phi$ , we need to determine  $\phi$  with high accuracy.

It is difficult to determine  $\phi$  in the quasi-two-dimensional foam, although  $\phi$  is one of the most important factors to describe the state of the foam [11,28]. In most of the previous studies the experiments were performed with a fixed  $\phi$  and the error of  $\phi$  has rarely been evaluated. When  $\phi$  is very low and the state is the dry foam, thin films of the liquid play important roles for coarsening of the bubbles and T1 events [19]. Thus, the thin film has usually been extracted as a line by image analyses. In this method,  $\phi$  cannot be determined accurately since the amount of the liquid is not measured. Meanwhile, the contact between the bubbles is crucial for the wet foam where  $\phi$  is close to the jamming point  $\phi_j$ . The contact area between the bubbles corresponds to the force strength, and the force chain can be observed in the jamming bubbles [3,11]. In this case, the liquid thin film is neglected and  $\phi$  is determined by the amount of the plateau region. The error in  $\phi$  is small near  $\phi_j$  since the contact area is small; however, the error becomes larger when  $\phi \ll \phi_j$ . Thus, the determination method of  $\phi$

has been chosen depending on the experimental situation. However, there are only a few methods in the determination of  $\phi$  that can be applied in a wide range of  $\phi$ , including the dry foam and the wet foam regimes. Furthermore, another problem in the quasi-two-dimensional foam is that the foam is projected into the two-dimensional plane and then  $\phi$  is also calculated as  $\phi_{2D}$ , which is a two-dimensional liquid fraction at the middle of the thickness. Practically, the foam is compressed by the sample chamber, and then the properties of the foam could be dependent on the thickness even though  $\phi_{2D}$  is the same (see Discussion). Thus  $\phi$  should be determined with high accuracy in order to study the  $\phi$  dependence of the states of the foam systematically.

Here, we investigate the bubble shape change and the motion of the bubbles simultaneously. First, we show the method for the determination of the liquid fraction  $\phi$ , which takes into consideration the three-dimensional geometry of the bubbles necessary in our experiment and shows the merits of using the three-dimensional liquid fraction  $\phi$  instead of  $\phi_{2D}$ . Then we show direct evidence of the relation between the dry-wet transition and the rearrangement.

## II. SAMPLE AND METHODS

Here we give some brief information about our data sets and refer to Ref. [27] for the detailed information. We used a solution in which 14% TTAB (tetradecyl trimethyl ammonium bromide) was mixed with deionized water. We adjusted the solution to control the interval time of the bubble collapse events by mixing 17% glycerol with the solution. The density of the solution was  $\rho = 1.1942 \text{ g/cm}^3$ . The foams are created by using a capillary glass tube equipped with an air pump. We sandwiched the foam by two glass plates and controlled the sample thickness  $h$  to  $h = 1 \text{ mm}$  by using a spacer. Then the sample chamber was sealed with silicon grease in order to prevent evaporation. The evaporation of the liquid estimated by measuring the weight of the sample was about 0.1% in the time interval of 16 000 s. The size of the entire foam was approximately 60 mm in diameter. The average value of the diameter of the bubbles was about 4 mm. In this condition, the foam in our sample chamber became one layer and can be regarded as quasi two dimensional. The number of the bubbles  $N$  is more than 200 in a small foam system and 1200 in a large foam system at  $t = 0$ . The bubbles collapse with time, which occurs mainly from the edge of the foam system, and thus  $N$  decreases with time (see Supplemental Material [29] video). We performed the same experiment nine times in order to confirm the reproducibility. The temperature was controlled by air conditioner at around 16 °C. We took images during the collapsing process of the bubbles by a digital video camera (Panasonic Co., HC-V520M) with a time interval of 1 s. We set the  $xy$  plane to an in-plane of the image and the  $z$  axis to the direction of the thickness of the sample chamber.

## III. RESULTS

### A. Determination of the liquid fraction

Figure 1 shows the images of the quasi-two-dimensional foam prepared in the present experimental setup. Figure 1(a1) is the image of  $t = 100 \text{ s}$  and the system is in the superdry

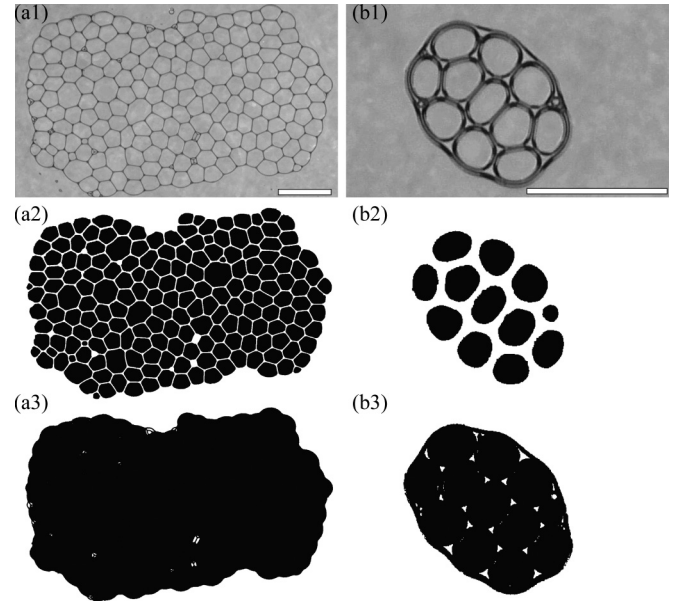


FIG. 1. Snapshots of the foam at (a1)  $t = 0 \text{ s}$  and (b1)  $t = 3000 \text{ s}$ . (a2) and (b2) are binarized images of (a1) and (b1) when the interface is regraded as the liquid phase. Meanwhile, (a3) and (b3) are the binarized images of (a1) and (b1) when the interface is regraded as the gas phase. The white bars in (a1) and (b1) correspond to 10 mm.

foam state. It is recognized that the liquid film separating the bubbles appears to be a thin line. Meanwhile, Fig. 1(b1) is the image of  $t = 3000 \text{ s}$  at which the system is in the wet foam state. The shape of the bubble becomes rounded and the liquid film becomes thicker. In the foam system, the thickness of the interface between the bubbles reflects nonuniform distribution of the liquid in the  $z$  direction. Figure 2(a) shows the image of  $t = 15000 \text{ s}$ , and this state is quite close to the jamming transition point. The bubbles contact each other only at the points. Figure 2(b) is a schematic image of the cross section in the  $z$  direction along the gray (yellow) line shown in Fig. 2(a). The gray and the white regions correspond to the liquid and the gas bubble, respectively. Roughly speaking, the thickness of the interface measured from the top reflects the roundness of the bubble in the  $z$  direction. According to the Laplace equation, the roundness is related to the pressure in the bubble [30]. The pressure in the bubble becomes lower with increasing  $\phi$  due to decreasing the contact area between the bubbles, and then the interface observed in the top view looks broad in the wet foam.

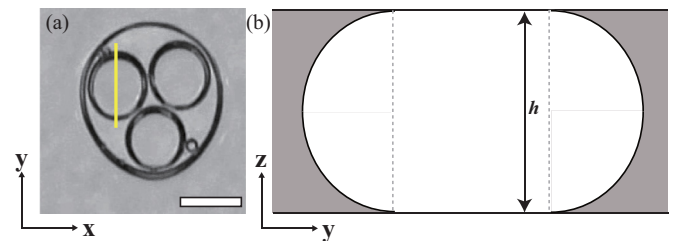


FIG. 2. (a) A snapshot of the foam at  $t = 15000 \text{ s}$ . The white bar corresponds to 4 mm. (b) Schematic image of the cross section in  $z$  direction at the yellow line shown in (a).

The quasi-two-dimensional foam is usually regarded as two-dimensional foam for qualitative analysis. To obtain the liquid fraction  $\phi_{2D}$  in the two-dimensional foam, the gas phase and the liquid phase are distinguished by a binarization. Due to the roundness of the interface in  $z$  direction, the definition of the binarization strongly affects the resulting value of  $\phi_{2D}$ . Figure 1(a2) is the binarized image of the dry foam shown in Fig. 1(a1), where the interface is regarded as the liquid phase (method A). The black and the white color correspond to the bubble and the liquid phase, respectively. Figure 1(a2) looks reproduced Fig. 1(a1). Meanwhile, Fig. 1(a3) is the binarized image of (a3), where the interface is regarded as the gas phase (method B). The whole system is regarded as the bubble region and it is clearly inappropriate. For the superdry foam, the method A is suitable rather than the method B. However, the situation becomes opposite for the wet foam. Figure 1(b2) is the binarized image of Fig. 1(b1) with method A. Each bubble is isolated in the image, although the bubbles actually contact each other. On the other hand, the contacts between the bubbles appear in Fig. 1(b3), which is obtained by using method B. Thus both method A and method B are not appropriate to use for the experiment in which  $\phi$  changes in a wide range, including the superdry foam and the wet foam.

We propose a method of the determination of the three-dimensional  $\phi$  instead of  $\phi_{2D}$  for our experiment. It is not so difficult to determine  $\phi = V_{\text{liquid}}/V_{\text{foam}}$  for a fixed  $\phi$ . When the foam is sandwiched in a chamber with the thickness  $h$ , the whole volume of the foam can be obtained as  $V_{\text{foam}} = S \times h$ , where  $S$  is the whole area of the foam obtained from the snapshot image. Meanwhile,  $V_{\text{liquid}}$  can be obtained by the weight of the system  $m$  and the density  $\rho$ . However, this method is not available for a long time experiment since we should seal our sample chamber immediately in order to prevent the evaporation of the liquid. We conceive a method for estimation of  $\phi$  which is applicable to a wide range of  $\phi$ . The volume of the liquid  $V_{\text{liquid}}$  can be regarded as constant since the evaporation of the liquid is negligible in our experiment. The error in the estimation of  $V_{\text{liquid}}$  from the image analysis mainly comes from the interface between the bubbles and the liquid. Thus we estimate  $V_{\text{liquid}}$  using the last image ( $t = 16000$  s) in our experiment when the number of the bubble and the area of the interface is the least. Since it is difficult to obtain the distribution of the liquid in  $z$  direction due to the complex refraction [28], we roughly estimate  $V_{\text{liquid}}$  as

$$V_{\text{liquid}} \approx 1 - \frac{\sum_j (S_{\text{in}}^j + S_{\text{out}}^j)h}{2}, \quad (1)$$

where  $S_{\text{in}}^j$  is the area of the bubble  $j$  inside the interface in the top view and  $S_{\text{out}}^j$  is the area including the interface area. To evaluate the validity of this estimation of  $V_{\text{liquid}}$ , we measure  $m$  and take a snapshot of an independent foam near the jamming point. Then we compare  $V_{\text{liquid}}$  estimated using Eq. (1) with  $V_{\text{liquid}}$  determined from the measurement of  $m$ . We find that  $V_{\text{liquid}}$  determined by the image analysis is in agreement with  $V_{\text{liquid}}$  from the weight within 10% of errors. Finally, we obtain  $\phi(t) = V_{\text{liquid}}/V_{\text{foam}}(t)$ , where  $V_{\text{foam}}(t) = S_{\text{foam}}(t)h$  and  $S_{\text{foam}}(t)$  is the area of the whole system of the foam at  $t$ . We show a time evolution of  $\phi$  calculated by the above method, shown as a triangle symbol in Fig. 3. For comparison, we

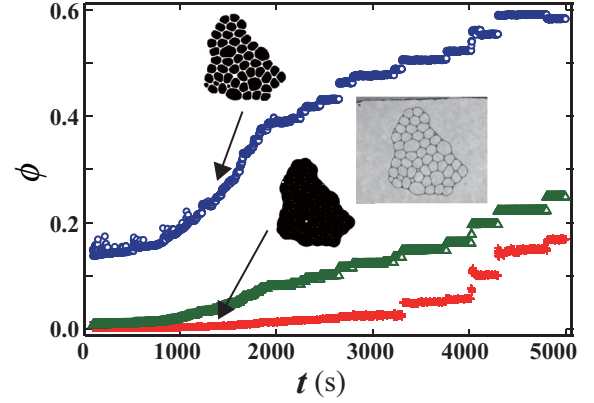


FIG. 3. Time evolution of the calculated  $\phi$ . The triangle symbol corresponds to the liquid fraction calculated by our method. The circle and the cross symbols correspond to the liquid fraction when the interface area is regarded as the liquid phase and as the gas phase, respectively. A snapshot of the foam at  $t = 1200$  s, the binarized image obtained by using method A, and the binarized image obtained by using method B are inserted.

also show  $\phi_{2D}$  when we regard the interface as the gas phase (cross) and as the liquid phase (circle). Near the jamming transition at  $t = 5000$  s,  $\phi = 0.18$  when the interface is regarded as the gas phase and it is close to  $\phi_{2D}$  of the jamming transition ( $\phi_{2D} \approx 0.16$ ). However,  $\phi_{2D} \approx 0$  below  $t = 1200$  s, even though the interface becomes thicker. (See the inset in Fig. 3.) Meanwhile,  $\phi_{2D} = 0.16$  even at  $t = 0$  when we regard the interface as the liquid phase (circle) and it is too large for the superdry foam. In addition,  $\phi_{2D} = 0.58$  at  $t = 5000$  s is much larger than  $\phi_{2D}$  at the jamming transition. The enormously large error comes from the large area of the interface and the amount of the liquid thin film between the bubbles is overestimated [28]. Thus it is suitable to apply the three-dimensional liquid fraction  $\phi$  for the range extended from the superdry foam to the wet foam regimes.

### B. Bubble size change during the collapsing process

Then we investigate the mean bubble size during the collapsing process. The bubble size is related to the osmotic pressure  $p$  and then the dynamics of the foam should be affected by the bubble size. Figure 4 shows the mean area of

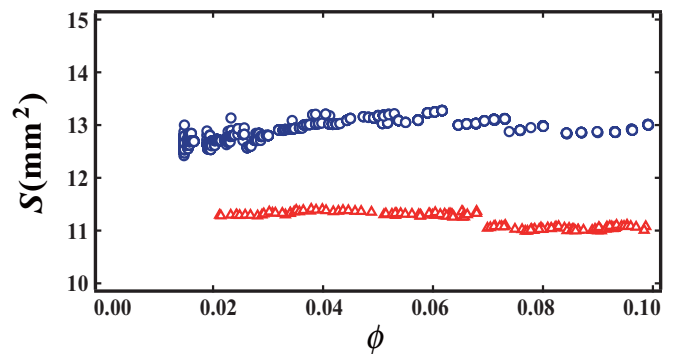


FIG. 4. The mean area of the bubbles for  $N > 200$  (circles) and for  $N > 1200$  (triangles) as a function of  $\phi$ . The mean areas of the bubbles are almost constant in both systems.



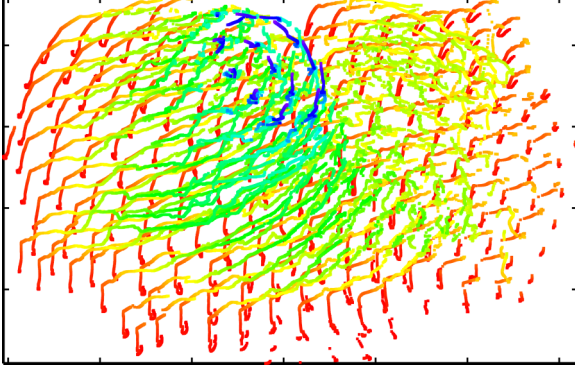


FIG. 5. Trajectories of all the bubbles as a function of time. Time increases from red ( $t = 0$  s) to blue color ( $t = 5000$  s).

the bubbles as a function of  $\phi$ . The mean area of the bubbles is almost constant. Thus the effect of the mean bubble size on the dynamics of the foam may be negligible in our experiments.

### C. Dynamical transition

Next, we investigate the dynamics of the foam during the collapsing process of the bubbles. We extract the shape of the each bubble using the inside curve of the interface. Although using the inside curve is not suitable for the determination of  $\phi$ , we can investigate the time evolution of the shapes and the locations of all bubbles. We obtain the coordinate of the center of mass of the bubble  $k$   $\mathbf{r}_k(t)$  from the image. Then we compute the general pattern tracking method. We calculate  $\Delta \mathbf{r}_{jk} = \mathbf{r}_j(t+1) - \mathbf{r}_k(t)$ . When  $|\Delta \mathbf{r}_{jk}| < 100 \mu\text{m}$ , the bubble  $k$  is the same as the bubble  $j$  and  $|\Delta \mathbf{r}_{jk}|$  is a moving distance of the bubble  $j$ . Then we obtain trajectories of all the bubbles using the coordinates of all the bubbles. Figure 5 shows all trajectories from  $t = 0$  s to  $t = 3000$  s. The color changes from red to blue represent the time evolution. Here, the case when we miss the tracking of the bubble is considered as below: (i) The case when the bubble disappears due to the collapse. A number of the disappeared bubbles  $N_c(t)$  is described as

$$N_c(t) = N_b(t) - N_b(t+1), \quad (2)$$

where  $N_b(t)$  is a total number of the bubbles at  $t$ . (ii) The case when the bubbles rearrange their positions. Some bubbles move over  $100 \mu\text{m}$  in the time interval of the tracking when the positional rearrangement occurs. In this case,  $N_b(t)$  remains constant. (iii) The case when a large deformation of the bubble occurs due to a T1 event. We observe the T1 events only a few times in the experiment and thus the number belonging to case (iii) is negligible. From (i)–(iii), we obtain

$$N_f(t) = N_a(t) + N_c(t), \quad (3)$$

where  $N_f(t)$  and  $N_a(t)$  are a number of the bubbles which we fail to track and a number of the bubbles which rearrange their positions. Then, we define a parameter  $P$  as

$$P(t) = N_a(t)/N_c(t) = N_f(t)/N_c(t) - 1. \quad (4)$$

$P$  represents the mean number of the bubbles which rearranged after one bubble collapsed, and  $P = 0$  means that no bubble rearranged when one bubble collapsed. Figure 6 shows the  $\phi$  dependence of  $P$ . For  $\phi < 0.055$ , we find  $P \approx 0.7$  in average,

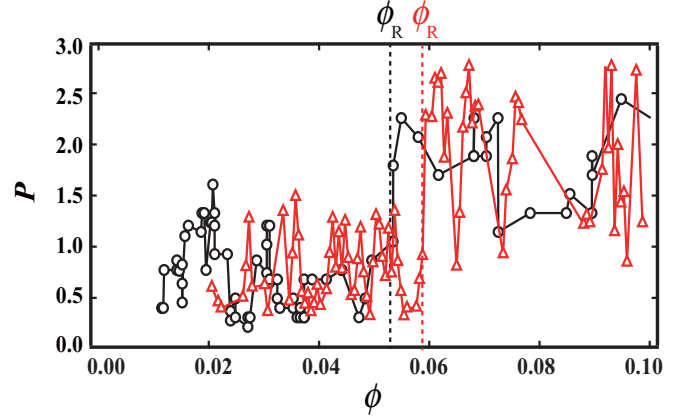


FIG. 6.  $P$  as a function of  $\phi$ .  $P$  corresponds to the number of the rearrangement per one-time collapse of a bubble.  $P$  drastically changes at  $\phi_R = 0.055$  for  $N > 200$  (circles) and  $\phi_R = 0.059$  for  $N > 1200$  (triangles).

and it means that the rearrangement rarely occurs when one bubble collapses. Meanwhile,  $P$  drastically increases at  $\phi = 0.055$  and  $P$  becomes approximately 2.5. It suggests that the rearrangement easily occurs for  $\phi > \phi_R$ , where  $\phi_R$  is a liquid fraction when the dynamical transition occurs.

### D. Transformation of bubble shape

Furthermore, we investigate the radius of the curvature  $r_{\text{inter}}$  at each point of the interface of the bubble in order to compare the rearrangement events with the change of the bubble shape, which is reported in Ref. [27]. We calculate  $r_{\text{inter}}$  by using the method proposed in Ref. [27]. The measurement of  $r_{\text{inter}}$  is not high accuracy; thus we use  $\beta$ , which is a ratio of the straight line to the circumference of the bubble. We regard the interface as the line when  $r_{\text{inter}} > 5 \text{ mm}$ , which is chosen as a value more than twice as large as the average radius of the bubble ( $\sim 2 \text{ mm}$ ).  $\beta$  is large when the bubble shape is close to polygonal, and vice versa.

Figure 7 shows  $\beta$  as a function of  $\phi$  and the dotted vertical line corresponds to  $\phi_R$ . We find that  $\beta$  decreases

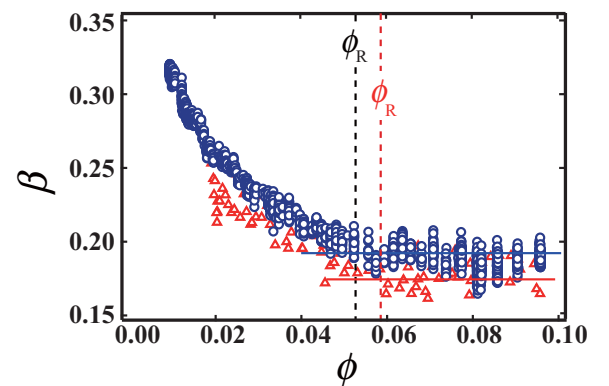


FIG. 7.  $\beta$  as a function of  $\phi$ .  $\beta$  is a ratio of the straight line to the circumference of the bubble. The dotted line corresponds to  $\phi = \phi_R$ .  $\phi$  dependence of  $\beta$  also changes at  $\phi_R = 0.055$  for  $N > 200$  (circles) and  $\phi_R = 0.059$  for  $N > 1200$  (triangles).

with increasing  $\phi$  below  $\phi = \phi_R$ , while  $\beta$  is almost constant for  $\phi > \phi_R$ . This means that the transition of the bubble shape occurs at  $\phi = \phi_R$ , and we consider that this transition corresponds to the dry-wet transition. Thus we consider that it is strong evidence for the relationship between the dry-wet transition and the rearrangement of the bubbles. In addition, the transition point  $\phi_R = 0.055$  in our measurement is consistent with the empirical criteria for the dry foam in the three-dimensional foam system, which is known as  $\phi \approx 0.05$ . This result is consistent with our previous result reported in Ref. [27], though  $\phi_R$  in this experiment is much smaller than that in the previous report. The difference of  $\phi_R$  comes from the difference of the determination method of  $\phi$ .

### E. Reproducibility

We perform the same experiment with the foam system consisting of over 1200 bubbles in order to confirm the relation between the dry-wet transition and the rearrangement of the bubbles. The bubble sizes,  $p$  and  $\beta$ , are shown in Figs. 4, 6, and 7. We find the same trend as the results in the system of  $N \approx 200$ . We also find a close relationship between the dry-wet transition and the rearrangement of the bubbles, although the foam shape at  $\phi_R$  is largely different at each experiment. Thus we consider the relationship between the dry-wet transition and the rearrangement of the bubbles is independent of the initial shape of the foam and the total number of the bubbles, at least when the mean bubble size is close.

In addition, we also investigate the  $h$  dependence of the state of the foam. The foam becomes double layer in the superdry state when  $h = 2$  mm, while the foam is unstable and collapses quickly when  $h = 0.5$  mm. (The mean diameter of the bubble is about 4 mm.) This means that the physical properties of the foam depend not only on  $\phi$  but also on  $h$ . We consider that three-dimensional  $\phi$  is a fundamental parameter for investigation of the  $h$  dependence of the foam state, rather than  $\phi_{2D}$ .

## IV. DISCUSSION

Here we explain a driving force for the rearrangement of the bubbles. The bubbles tend to collapse not in the center but from the edge of the system. When one bubble located at the edge of the foam collapses, the local roughness of the foam system becomes larger. Then the anisotropic surface tension induced by the local roughness drives the rearrangement of the bubbles.

Finally, we discuss the relation between the rearrangement and the change of  $\partial\beta/\partial\phi$  at  $\phi_R$ .  $\beta$ , which is the ratio of the straight line to the circumference of the bubble, is large when the bubbles are strongly packed. That is,  $\beta$  reflects the osmotic pressure  $p$ . Figure 7 suggests that  $p$  decreases with increasing  $\phi$  for  $\phi < \phi_R$ , while  $p$  becomes almost constant for  $\phi > \phi_R$ . This means that the rearrangement suppresses the change of  $p$ . Further investigation of the relation between  $p$  and  $\phi$  is needed.

## V. SUMMARY

We show the utility of the three-dimensional liquid fraction  $\phi$  from the superdry foam to the wet foam, while  $\phi_{2D}$  cannot be applied in the wide range of  $\phi$ . Then we simultaneously investigate the dynamical and the statical change during the collapsing process of the bubbles in which  $\phi$  changes continuously. We trace every bubble and find that the rearrangement occurs for  $\phi > \phi_R$ . We also find that the  $\phi$  dependence of the bubble shape changes at  $\phi = \phi_R$ . We consider it to be a direct evidence for the relation between the dry-wet transition and the rearrangement of the bubbles.

## ACKNOWLEDGMENTS

N.O. was supported by JSPS KAKENHI (Contract No. 17K14356). R.K. was also supported by JSPS KAKENHI (Contracts No. 16K13865 and No. 17H02945).

- 
- [1] A. J. Liu and S. R. Nagel, *Jamming and Rheology* (Taylor & Francis, London, 2001).
  - [2] A. J. Liu and S. R. Nagel, *Nature (London)* **396**, 21 (1998).
  - [3] K. W. Desmond, P. J. Younge, D. Chen, and E. R. Weeks, *Soft Matter* **9**, 3424 (2013).
  - [4] T. S. Majmudar, M. Sperl, S. Luding, and R. P. Behringer, *Phys. Rev. Lett.* **98**, 058001 (2007).
  - [5] M. Schöter, S. Nägele, C. Radin, and H. L. Swinney, *Europhys. Lett.* **78**, 44004 (2007).
  - [6] P. Olsson and S. Teitel, *Phys. Rev. Lett.* **99**, 178001 (2007).
  - [7] J. D. Bernal and J. Mason, *Nature (London)* **188**, 910 (1960).
  - [8] G. D. Scott and D. M. Kilgour, *J. Phys. D: Appl. Phys.* **2**, 863 (1969).
  - [9] A. Donev, F. H. Stillinger, and S. Torquato, *Phys. Rev. Lett.* **95**, 090604 (2005).
  - [10] R. Kurita and E. R. Weeks, *Phys. Rev. E* **82**, 011403 (2010).
  - [11] G. Katgert and M. van Hecke, *Europhys. Lett.* **92**, 34002 (2010).
  - [12] J. Lauridsen, M. Twardos, and M. Dennin, *Phys. Rev. Lett.* **89**, 098303 (2002).
  - [13] B. Dollet and C. Raufaste, *C. R. Phys.* **15**, 731 (2014).
  - [14] B. Dollet and F. Graner, *J. Fluid Mech.* **585**, 181 (2007).
  - [15] G. Katgert, B. P. Tighe, and M. van Hecke, *Soft Matter* **9**, 9739 (2013).
  - [16] W. Drenckhan and S. Hutzler, *Adv. Colloid Interface Sci.* **224**, 1 (2015).
  - [17] R. Höhler, Y. Y. C. Sang, E. Lorenceau, and S. Cohen-Addad, *Langmuir* **24**, 418 (2008).
  - [18] I. Fortuna, G. L. Thomas, R. M. C. de Almeida, and F. Graner, *Phys. Rev. Lett.* **108**, 248301 (2012).
  - [19] D. L. Weaire and S. Hutzler, *The Physics of Foams* (Clarendon Press, Oxford, 1999).
  - [20] D. Weaire, F. Bolton, T. Herdtle, and H. Aref, *Philos. Mag. Lett.* **66**, 293 (1992).
  - [21] T. Okuzono and K. Kawasaki, *Phys. Rev. E* **51**, 1246 (1995).
  - [22] M. Dennin, *Phys. Rev. E* **70**, 041406 (2004).

- [23] D. J. Durian, *Phys. Rev. Lett.* **75**, 4780 (1995).
- [24] A. Abdel Kader and J. C. Earnshaw, *Phys. Rev. Lett.* **82**, 2610 (1999).
- [25] R. Lespiat, S. Cohen-Addad, and R. Höhler, *Phys. Rev. Lett.* **106**, 148302 (2011).
- [26] M. Le Merrer, S. Cohen-Addad, and R. Höhler, *Phys. Rev. Lett.* **108**, 188301 (2012).
- [27] Y. Furuta, N. Oikawa, and R. Kurita, *Sci. Rep.* **6**, 37506 (2016).
- [28] A. van der Net, L. Blondel, A. Saugey, and W. Drenckhan, *Colloids Surf. A: Physicochem. Eng. Aspects* **309**, 159 (2007).
- [29] See Supplemental Material at <http://link.aps.org/supplemental/10.1103/PhysRevE.95.062613> for a video of the collapse process of the foam with  $N > 1200$ .
- [30] The contrast of the image at the interface is due to the refraction at the boundary between the liquid and the bubble. Therefore the thickness of the interface actually observed is thicker than the real thickness (see also Ref. [26]).